

Supporting information

Cu₅FeS₄ quantum dots as single-component photo-assisted electrocatalyst for efficient hydrogen evolution

Dongxu Zhang,^a Yanhong Liu,^{*a} Longhua Li,^a Di Li,^a Tianyao Jiang,^a Hui Huang,^b Deli Jiang,^{*a} Zhenhui Kang,^{*bc} and Baodong Mao^{*a}

^a*School of Chemistry and Chemical Engineering, Jiangsu University, 301 Xuefu Road, Zhenjiang 212013, China*

^b*Institute of Functional Nano and Soft Materials (FUNSOM), Jiangsu Key Laboratory for Carbon-based Functional Materials and Devices, Soochow University, 199 Ren'ai Road, Suzhou 215123, China*

^c*Macao Institute of Materials Science and Engineering (MIMSE), MUST-SUDA Joint Research Center for Advanced Functional Materials, Macau University of Science and Technology, Taipa 999078, Macao, China*

**Corresponding authors E-mail: liuyh@ujs.edu.cn (Y.L.); dlj@ujs.edu.cn (D.J.); zhkang@suda.edu.cn (Z.K.); maobd@ujs.edu.cn (B.M.).*

Electrochemical Measurements

All the electrochemical measurements were performed with a CHI 760E electrochemical analyzer (CH Instruments, Inc., Shanghai) in a standard three-electrode system with a rate of 5 mV s^{-1} . Typically, the catalysts grown on Nickel foam (NF) were employed as working electrode, Hg/HgO as reference electrode, and graphite rod as the counter electrode for HER tests in 1.0 M KOH electrolyte, in which the NF was ultrasonically treated in acetone and ethanol solution and followed by washing with distilled water. Notedly, Ag/AgCl and Hg/HgO are used as reference electrodes when electrolyte pH=3 and 7, respectively. The potentials vs. reversible hydrogen electrode (RHE) were converted from the reference scale by using the following equations: $E_{(RHE)} = E_{(Hg/HgO)} + 0.098 \text{ V} + 0.059 \times \text{pH}$ and $E_{(RHE)} = E_{(Ag/AgCl)} + 0.1976 \text{ V} + 0.059 \times \text{pH}$.

The double-layer capacitance (C_{dl}) was measured in 1.0 M KOH solution by cyclic voltammetry (CV) with scanning rates of 10-100 mV/s in the potential range from 0.72 to 0.82 V versus RHE. Electrochemical impedance spectra (EIS) and Mott-Schottky plots of the samples were measured in three different electrolytes, including 0.5 M H_2SO_4 , 1.0 M PBS and 1.0 M KOH.

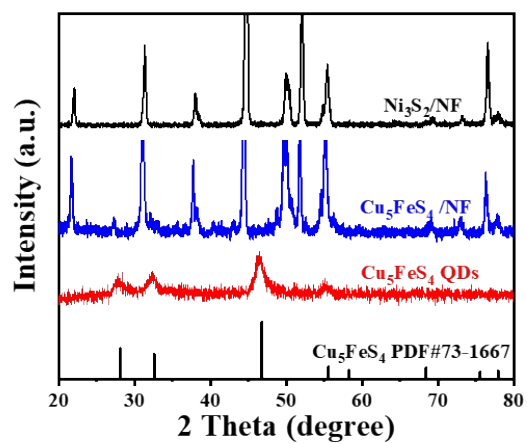


Fig. S1 The XRD patterns of Cu₅FeS₄ QDs (JCPDS no. 73-1667), Cu₅FeS₄/NF and Ni₃S₂/NF.

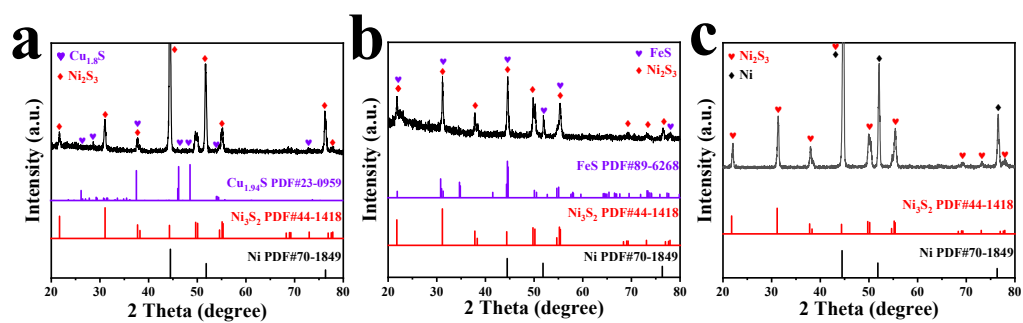


Fig. S2 The XRD patterns of (a) Cu_{2-x}S (JCPDS no. 23-0959), (b) FeS (JCPDS no. 89-6268) and (c) Ni₃S₂ (JCPDS no. 44-1418) samples.

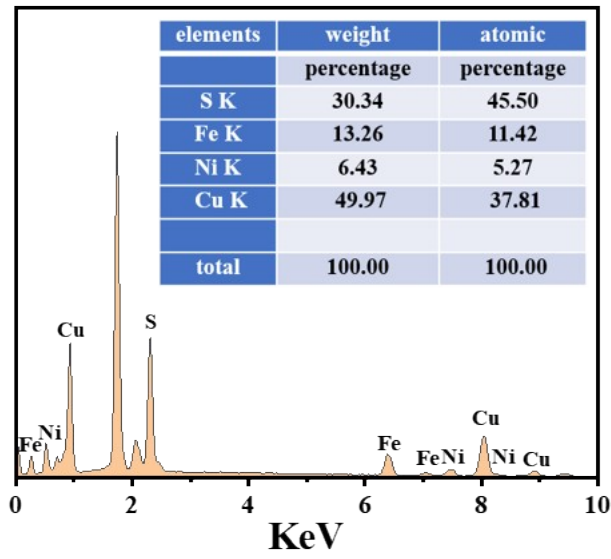


Fig. S3 EDX spectrum of the Cu₅FeS₄ QDs.

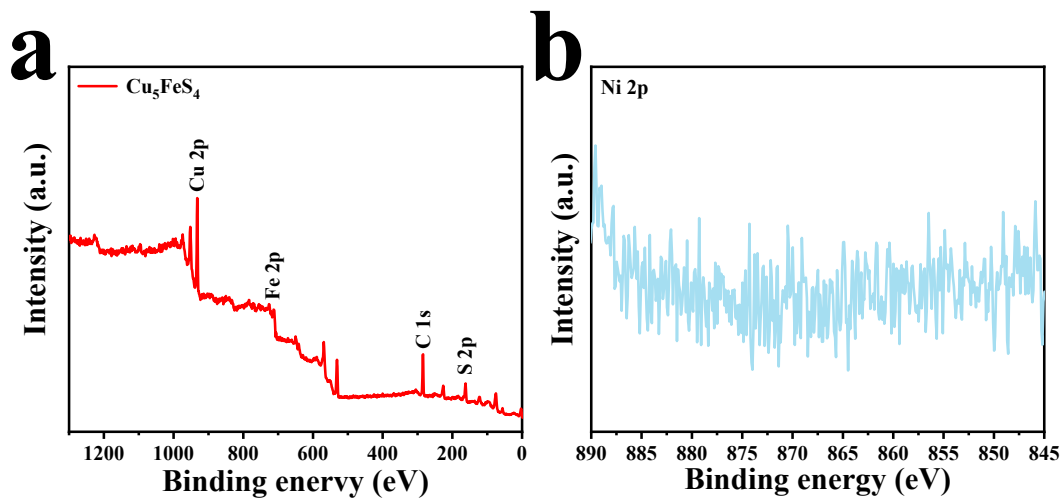


Fig. S4 XPS spectra of Cu_5FeS_4 QDs: (a) survey and (b) Ni 2p.

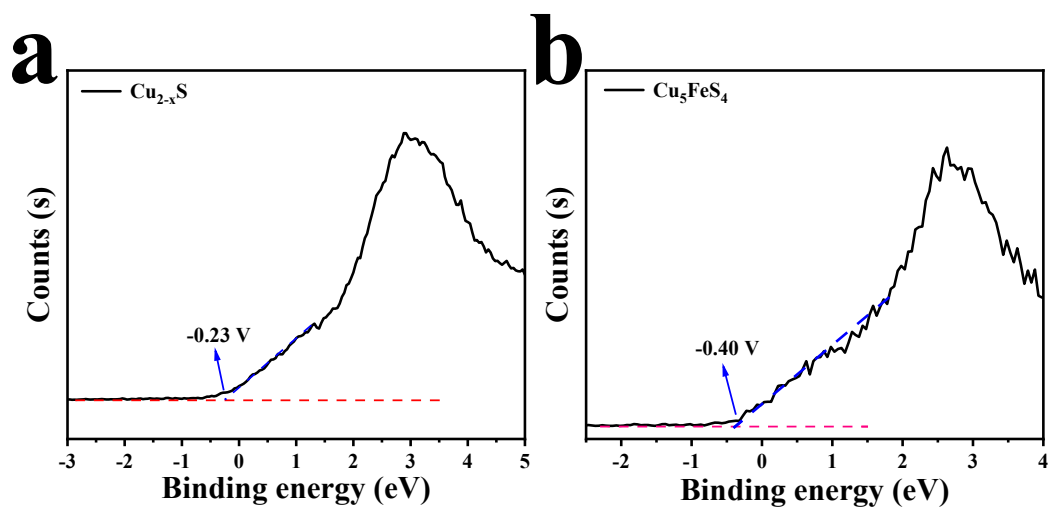


Fig. S5 The XPS valence band spectra of (a) Cu_{2-x}S QDs and (b) Cu_5FeS_4 .

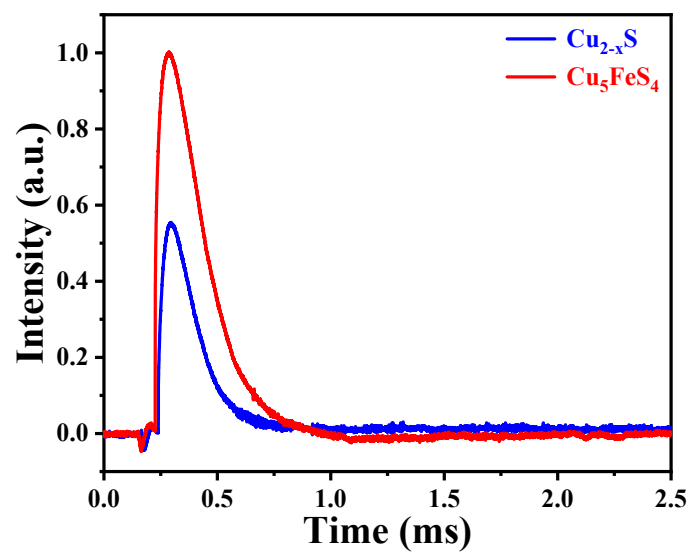


Fig. S6 TPV relaxation curves of Cu_{2-x}S QDs and Cu_5FeS_4 .

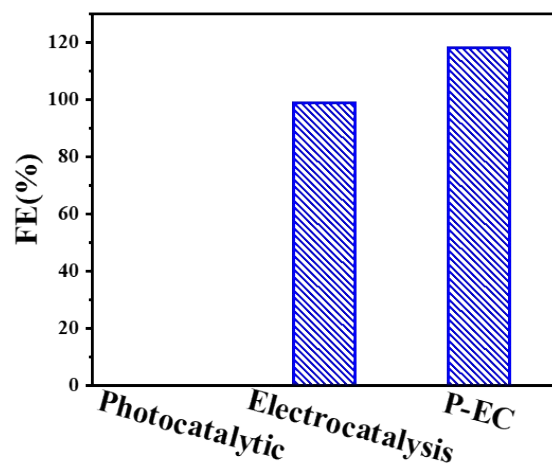


Fig. S7 The FE of electrocatalytic, photocatalytic and P-EC hydrogen production.

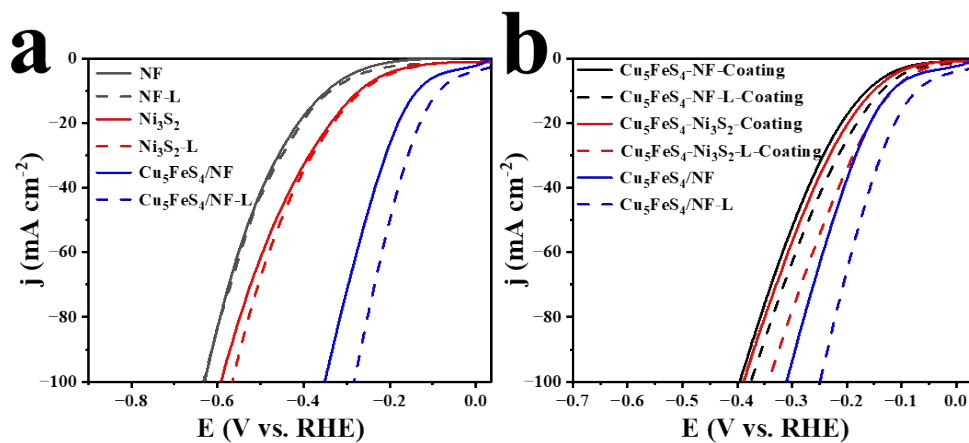


Fig. S8 The electrocatalytic and P-EC HER activity of (a) NF, NF-L, Ni₃S₂, Ni₃S₂-L, Cu₅FeS₄/NF and Cu₅FeS₄/NF-L and (b) Cu₅FeS₄-NF, Cu₅FeS₄-NF-L, Cu₅FeS₄-Ni₃S₂, Cu₅FeS₄-Ni₃S₂-L, Cu₅FeS₄/NF and Cu₅FeS₄/NF-L.

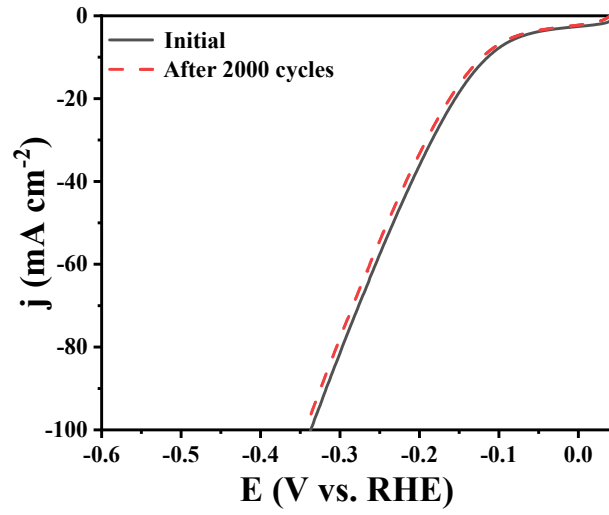


Fig. S9 Polarization curves of Cu₅FeS₄/NF before and after 2000 CV cycles under dark.

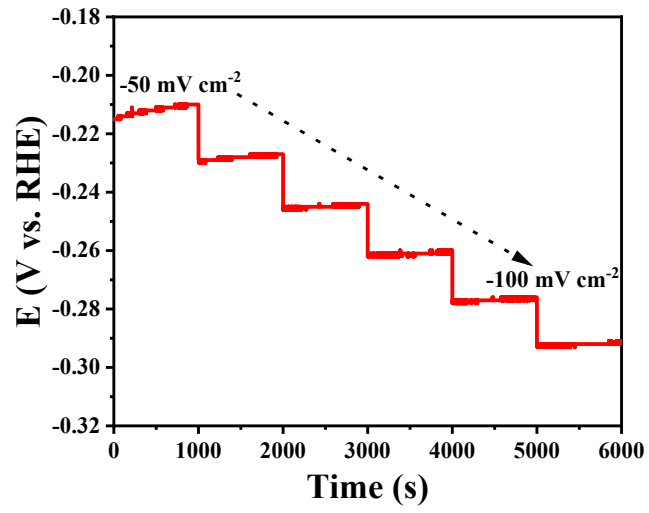


Fig. S10 The multi-current-process i-t curve of Cu₅FeS₄/NF under dark.

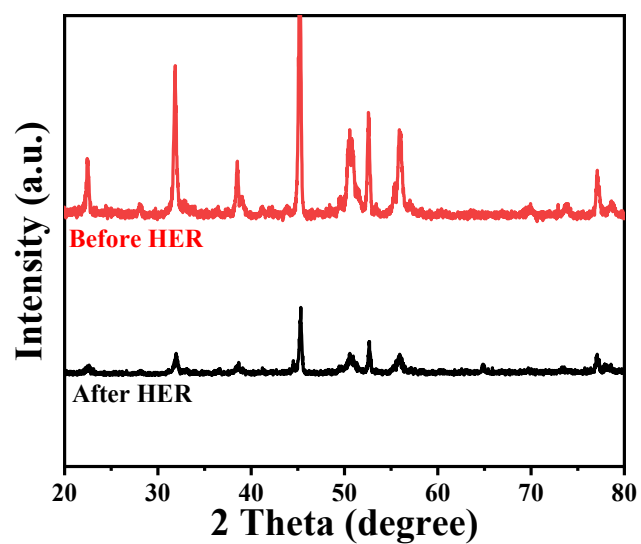


Fig. S11 XRD patterns of Cu₅FeS₄/NF before and after P-EC catalysis test of 20 h under continuous light irradiation.

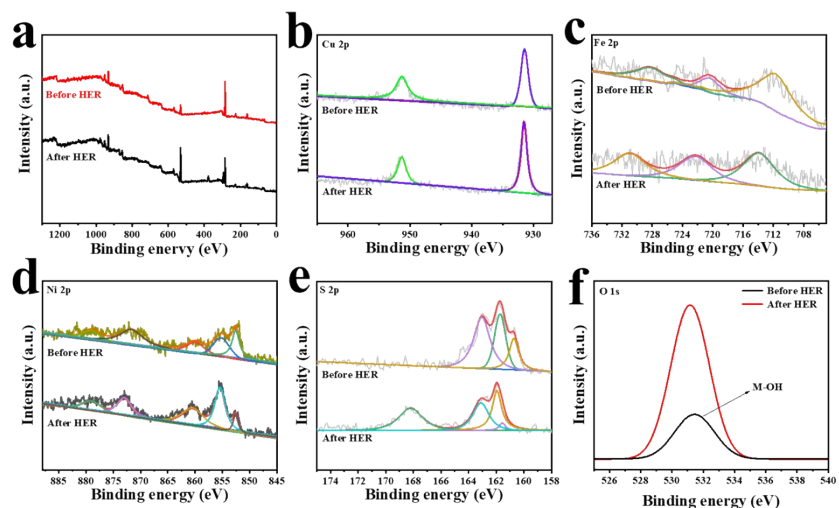


Fig. S12 XPS of $\text{Cu}_5\text{FeS}_4/\text{NF}$ before and after P-EC test of 20 h under continuous light irradiation: (a) survey, (b) Cu 2p, (c) Fe 2p, (d) Ni 2p, (e) S 2p and (f) O 1s.

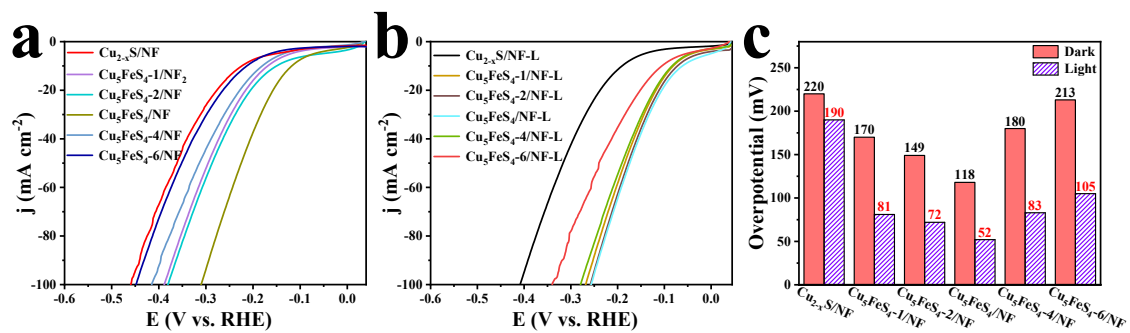


Fig. S13 Polarization curves of (a) electrocatalytic and (b) P-EC with different Cu/Fe ratios. (c) The corresponding overpotentials at current density of 10 mA cm⁻² for different electrodes.

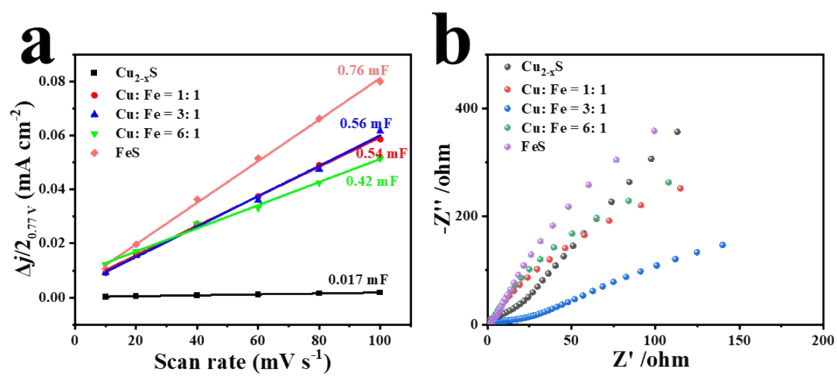


Fig. S14 (a) C_{dl} and (b) EIS patterns of the catalysts different Cu/Fe ratios.

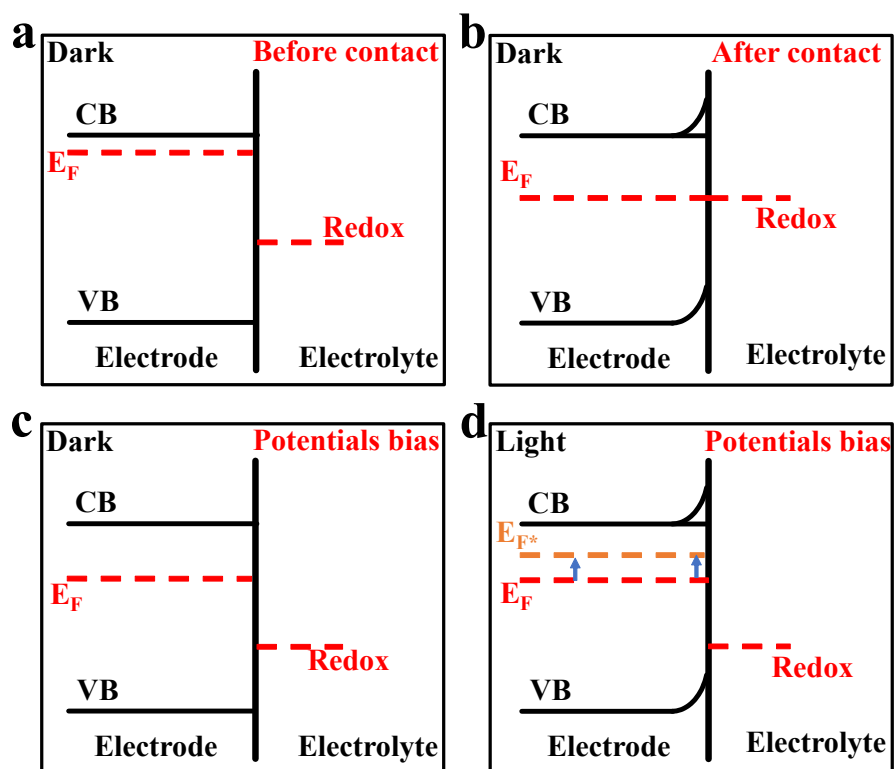


Fig. S15 Conduction and Valence band behaviour in electrode and electrolyte interface: (a) before contact, (b) after contact, (c) and (d) under potential bias without and with light, respectively.

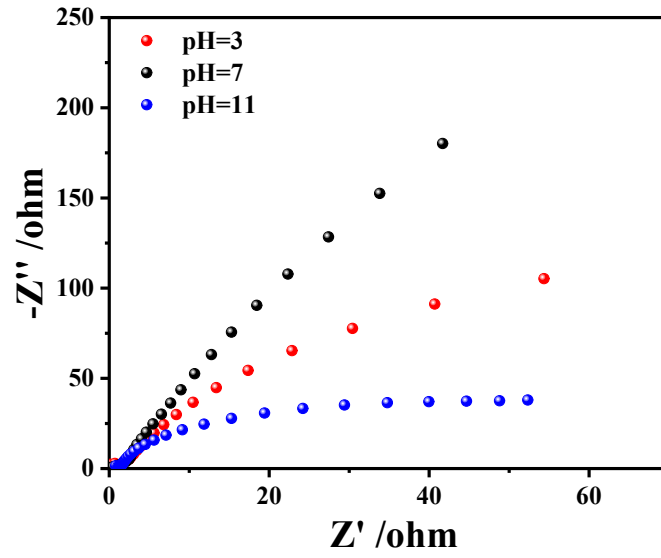


Fig. S16 EIS patterns of $\text{Cu}_5\text{FeS}_4/\text{NF}$ in three different electrolytes (pH = 3, 7 and 11).

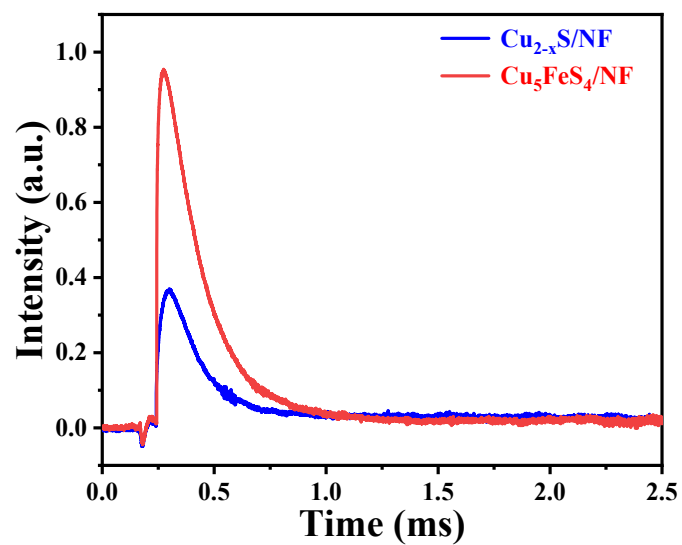


Fig. S17 TPV relaxation curves of $\text{Cu}_{2-x}\text{S}/\text{NF}$ and $\text{Cu}_5\text{FeS}_4/\text{NF}$.

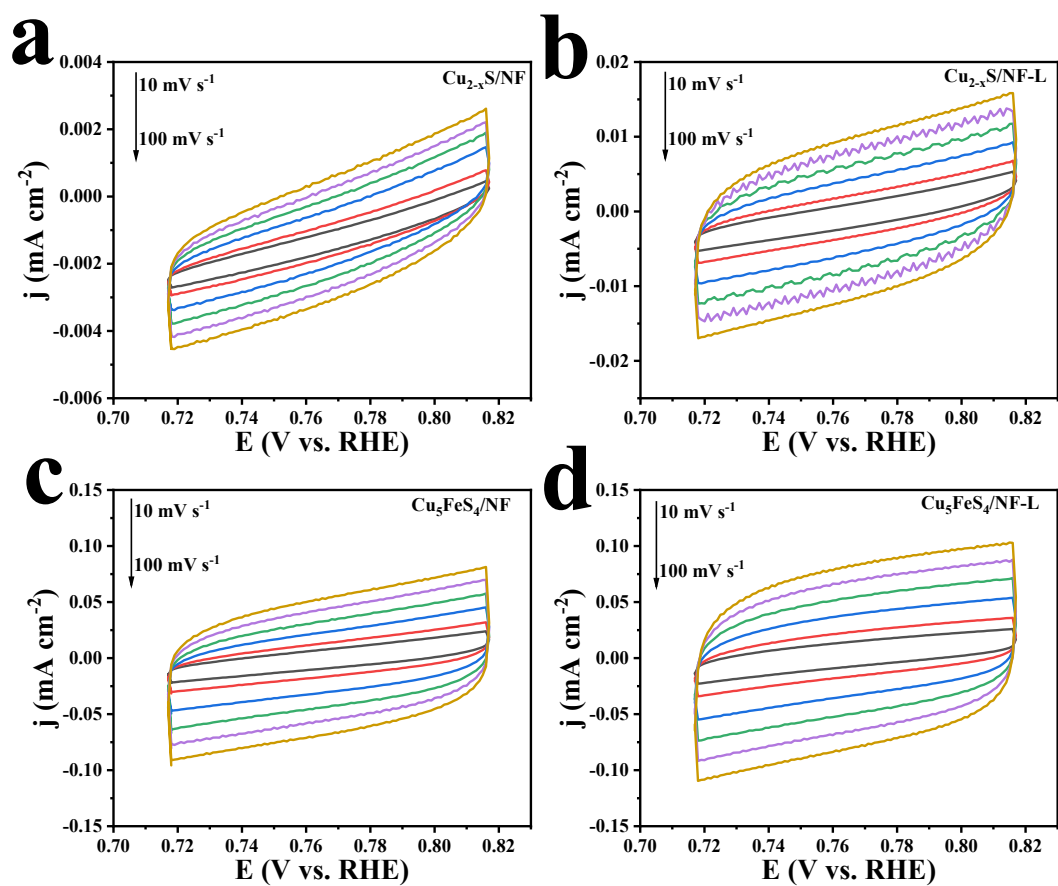


Fig. S18 CV curves at different scan rates of $\text{Cu}_{2-x}\text{S}/\text{NF}$ without (a) and with light (b); CV curves at different scan rates of $\text{Cu}_5\text{FeS}_4/\text{NF}$ without (c) and with light (d).

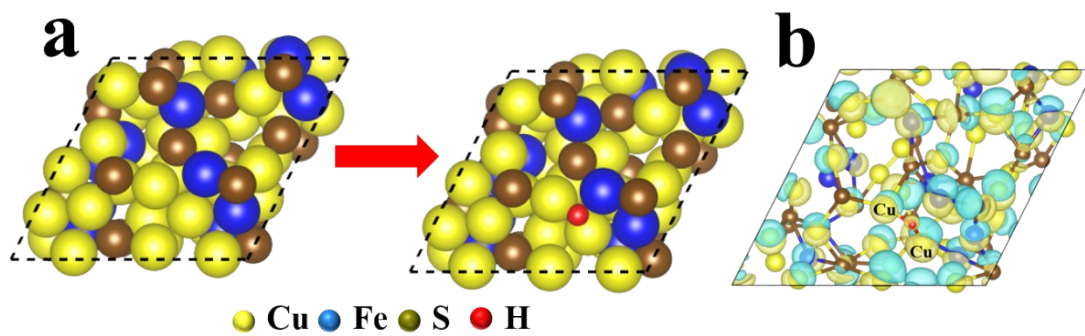


Fig. S19 (a) Top view of H^+ adsorption and (b) charge density difference of Cu_5FeS_4 QDs without light.

Table S1 HER performance comparison between Cu₅FeS₄/NF-L in our work and other cheap transition metal catalysts reported previously.

| Catalysts | Electrolyte | Overpotential at 10 mA cm ⁻² (mV) | Refs. |
|--|--------------------------------------|---|------------------|
| Cu₅FeS₄/NF-L | 1M KOH | 52 | This work |
| TiS _{2-x} /NiS | 1M KOH | 63 | 1 |
| Ni-Fe-P-Ni ₃ S ₂ /NF | 1M KOH | 65 | 2 |
| MoS ₂ -RGO | 0.5 M H ₂ SO ₄ | 66 | 3 |
| N-NiMoS | 0.1 M KOH | 68 | 4 |
| CdS@Co ₈ S ₉ /Ni ₃ S ₂ | 1M KOH | 69.6 | 5 |
| Fe _x Ni _{3-x} S ₂ @NF | 1M KOH | 72 | 6 |
| N-NiS ₂ /CoS ₂ | 1M KOH | 73 | 7 |
| NiFeCoS _x @FeNi ₃ | 1M KOH | 88 | 8 |
| N-NiMoO ₄ /NiS ₂ | 1M KOH | 99 | 9 |
| NiSe-Ni _{0.85} Se | 1M KOH | 101 | 10 |
| Fe-Ni ₃ S ₂ @FeNi ₃ | 1M KOH | 105 | 11 |
| B-Fe ₇ S ₈ /FeS ₂ | 1M KOH | 113 | 12 |
| W-NiO/NiS ₂ | 1M KOH | 116 | 13 |
| NiCo ₂ S ₄ /Ni ₃ S ₂ | 1M KOH | 127 | 14 |
| Fe-CoMoS | 1M KOH | 137 | 15 |
| Co _{0.9} S _{0.58} P _{0.42} | 1M KOH | 141 | 16 |
| FeS | 1M KOH | 142 | 17 |
| Ni ₃ S ₂ | 1M KOH | 147 | 18 |
| Co ₉ S ₈ -MoS ₂ /N-CNAs@CNFs | 1M KOH | 163 | 19 |
| Fe _{0.95-x} Ni _x S _{1.05} | 1M KOH | 263 | [0] |

Table S2 The R_{ct} values of Cu_5FeS_4/NF in different electrolytes with/without light.

| Samples | Dark ($\Omega\text{ cm}^2$) | Light ($\Omega\text{ cm}^2$) |
|---------|-------------------------------|--------------------------------|
| pH=3 | 320.5 | 155.6 |
| pH=7 | 478.9 | 424.2 |
| pH=11 | 270.7 | 73.8 |

Table S3 Fitting parameters of the EIS data of different samples using the equivalent circuit in the inset of Fig. 5f.

| Samples | R_s ($\Omega \text{ cm}^2$) | R_{ct} ($\Omega \text{ cm}^2$) |
|---------------------------------------|---------------------------------|------------------------------------|
| $\text{Cu}_{2-x}\text{S}/\text{NF}$ | 112.3 | 1165.3 |
| $\text{Cu}_{2-x}\text{S}/\text{NF-L}$ | 28.8 | 283.9 |
| $\text{Cu}_5\text{FeS}_4/\text{NF}$ | 19.4 | 268.8 |
| $\text{Cu}_5\text{FeS}_4/\text{NF-L}$ | 1.3 | 24.9 |

References:

- 1 J. Wu, W. Zhong, C. Yang, W. Xu, R. Zhao, H. Xiang, Q. Zhang, X. Li and N. Yang, *Appl. Catal., B*, 2022, **310**, 121332.
- 2 Z. Li, K. Wang, X. Tan, X. Liu, G. Wang, G. Xie and L. Jiang, *Chem. Eng. J.*, 2021, **424**, 130390.
- 3 X. Gao, J. Qi, S. Wan, W. Zhang, Q. Wang and R. Cao, *Small* 2018, **14**, 1803361
- 4 C. Huang, L. Yu, W. Zhang, Q. Xiao, J. Zhou, Y. Zhang, P. An, J. Zhang and Y. Yu, *Appl. Catal., B*, 2020, **276**, 119137.
- 5 F. Si, C. Tang, Q. Gao, F. Peng, S. Zhang, Y. Fang and S. Yang, *J. Mater. Chem. A*, 2020, **8**, 3083-3096.
- 6 B. Fei, Z. Chen, J. Liu, H. Xu, X. Yan, H. Qing, M. Chen and R. Wu, *Adv., Energy Mater.*, 2020, **10**, 2001963.
- 7 B. Qiu, Y. Zhang, X. Guo, Y. Ma, M. Du, J. Fan, Y. Zhu, Z. Zeng and Y. Chai, *J. Mater. Chem. A*, 2022, **10**, 719-725.
- 8 J. Shen, Q. Li, W. Zhang, Z. Cai, L. Cui, X. Liu and J. Liu, *J. Mater. Chem. A*, 2022, **10**, 5442-5451.
- 9 L. An, J. Feng, Y. Zhang, R. Wang, H. Liu, G.-C. Wang, F. Cheng and P. Xi, *Adv. Funct. Mater.*, 2019, **29**, 1805298.
- 10 Y. Chen, Z. Ren, H. Fu, X. Zhang, G. Tian and H. Fu, *Small*, 2018, **14**, 1800763.
- 11 W. Zhang, Q. Jia, H. Liang, L. Cui, D. Wei and J. Liu, *Chem. Eng. J.*, 2020, **396**, 125315.
- 12 J. Wu, Q. Zhang, K. Shen, R. Zhao, W. Zhong, C. Yang, H. Xiang, X. Li and N. Yang, *Adv. Funct. Mater.*, 2021, **32**, 2107802.
- 13 H. Wang, T. Liu, K. Bao, J. Cao, J. Feng and J. Qi, *J. Colloid Interface Sci.*, 2020, **562**, 363-369.
- 14 X. Zhao, H. Liu, Y. Rao, X. Li, J. Wang, G. Xia and M. Wu, *ACS Sust. Chem. Engin.*, 2018, **7**, 2610-2618.
- 15 Y. Guo, X. Zhou, J. Tang, S. Tanaka, Y.V. Kaneti, J. Na, B. Jiang, Y. Yamauchi, Y. Bando and Y. Sugahara, *Nano Energy*, 2020, **75**, 104913.
- 16 Z. Dai, H. Geng, J. Wang, Y. Luo, B. Li, Y. Zong, J. Yang, Y. Guo, Y. Zheng, X.

- Wang and Q. Yan, *ACS Nano*, 2017, **11**, 11031-11040.
- 17 G. Zhou, Y. Shan, L. Wang, Y. Hu, J. Guo, F. Hu, J. Shen, Y. Gu, J. Cui, L. Liu and X. Wu, *Nat. Commun.*, 2019, **10**, 399.
- 18 X. Shi, X. Ling, L. Li, C. Zhong, Y. Deng, X. Han and W. Hu, *J. Mater. Chem. A*, 2019, **7**, 23787-23793.
- 19 W. Zhang, X. Zhao, Y. Zhao, J. Zhang, X. Li, L. Fang and L. Li, *ACS Appl. Mater. Interfaces*, 2020, **12**, 10280-10290.
- 20 Z. Jing, Q. Zhao, D. Zheng, L. Sun, J. Geng, Q. Zhou and J. Lin, *J. Mater. Chem. A*, 2020, **8**, 20323-20330.